Inorg. Chem. **2007**, *46*, 10840–10849

Effect of Axial Ligands and Macrocyclic Structure on Redox Potentials and Electron-Transfer Mechanisms of Sn(IV) Porphyrins

Zhongping Ou,[†,‡] Wenbo E,[‡] Weihua Zhu,[†,‡] Pall Thordarson,[§] Paul J. Sintic,[§] Maxwell J. Crossley,[§] and Karl M. Kadish*[,‡]

Department of Applied Chemistry, Jiangsu University, Zhenjiang 212013, China, Department of Chemistry, University of Houston, Houston, Texas 77204-5003, and School of Chemistry, The University of Sydney, Sydney, NSW 2006, Australia

Received August 14, 2007

The electrochemical properties of dichloro- and dihydroxo-Sn(IV) porphyrins with three different macrocycles were examined in CH_2Cl_2 containing 0.1 or 0.2 M tetra-*n*-butylammonium perchlorate as supporting electrolyte. The investigated compounds are represented as (TPP)SnX_2, (P)$Sn(X)_2$, and (PQ)$Sn(X)_2$, where TPP = 5,10,15,20-tetraphenylporphyrin, P = 5,10,15,20-tetrakis(3,5-di-*tert*-butylphenyl)porphyrin, PQ = 5,10,15,20-tetrakis(3,5-di-*tert*-butylphenyl)quinoxalino[2,3-*b*′]porphyrin, and X = Cl or OH. Each porphyrin can be electroreduced in two one-electron-transfer steps with the half-wave potentials and stability of the eletroreduced compounds being dependent upon the type of coordinated axial ligand and specific macrocyclic structure. All reductions of (TPP)$Sn(OH)_2$, (P)$Sn(OH)_2$, and (PQ)$Sn(OH)_2$ are reversible under the given experimental conditions and lead to the expected porphyrin π-anion radicals and dianions, which were characterized by thin-layer UV–vis spectroelectrochemistry. This contrasts with what occurs upon the reduction of (PQ)$SnCl_2$, which undergoes a chemical reaction with trace H_2O in solution, leading to the formation of (PQ)$Sn(OH)_2$ as well as to a protonated form of the quinoxalinoporphyrin, (PQH)$Sn(OH)_2$, under the application of an applied potential. A protonation of the Q group breaks the conjugation between the fused quinoxaline unit and the porphyrin macrocycle, thus effectively giving a compound whose reduction properties resemble that of the metalloporphyrin in the absence of the fused ring. The electrooxidation of each neutral Sn(IV) porphyrin was also investigated, and the effect of axial ligand and fused quinoxaline ring on the redox potentials and products of electron transfer are discussed.

Introduction

Numerous Sn(IV) porphyrins have been synthesized and characterized,[1−29] leading to their possible use in a variety of applications,[1−16] including molecular recognition,[3] supramolecular chemistry,[2,5,7] and as components of photocatalytic devices[13] and nanomaterials.[9−16] A knowledge of the redox potentials and mechanisms of the electron transfer for the oxidation and reduction of these molecules is crucial

* To whom correspondence should be addressed. E-mail: kkadish@uh.edu.
† Jiangsu University.
‡ University of Houston.
§ The University of Sydney.

(1) Kumar, A. A.; Giribabu, L.; Reddy, D. R.; Maiya, B. G. *Inorg. Chem.* **2001**, *40*, 6757−6766.
(2) Maiya, B. G.; Bampos, N.; Kumar, A. A.; Feeder, N.; Sanders, J. K. M. *New J. Chem.* **2001**, *25*, 797−800.
(3) Crossley, M. J.; Thordarson, P.; Wu, R. A. S. *J. Chem. Soc., Perkin Trans. 1* **2001**, 2294−2302.
(4) Brotherhood, P. R.; Wu, R. A. S.; Turner, P.; Crossley, M. J. *Chem. Commun.* **2007**, 225−227.
(5) Langford, S. J.; Woodward, C. P. *CrystEngComm* **2007**, *9*, 218−221.
(6) Langford, S. J.; Latter, M. J.; Beckmann, J. *Inorg. Chem. Commun.* **2005**, *8*, 920−923.
(7) Langford, S. J.; Lau, V.-L.; Lee, M. A. P.; Lygris, E. *J. Porphyrins Phthalocyanines* **2002**, *6*, 748−756.
(8) Fallon, G. D.; Langford, S. J.; Lee, M. A. P.; Lygris, E. *Inorg. Chem. Commun.* **2002**, *5*, 715−718.
(9) Song, X.-Z.; Jia, S.-L.; Miura, M.; Ma, J.-G.; Shelnutt, J. A. *J. Photochem. Photobiol., A* **1998**, *113*, 233−241.
(10) Song, Y.; Yang, Y.; Medforth, C. J.; Pereira, E.; Singh, A. K.; Xu, H.; Jiang, Y.; Brinker, C. J.; van Swol, F.; Shelnutt, J. A. *J. Am. Chem. Soc.* **2004**, *126*, 635−645.
(11) Wang, Z.; Medforth, C. J.; Shelnutt, J. A. *J. Am. Chem. Soc.* **2004**, *126*, 16720−16721. Wang, Z.; Medforth, C. J.; Shelnutt, J. **2004**, *126*, 15954−15955.
(12) Wang, Z.; Li, Z.; Medforth, C. J.; Shelnutt, J. A. *J. Am. Chem. Soc.* **2007**, *129*, 2440−2441.
(13) Song, Y.; Steen, W. A.; Pena, D.; Jiang, Y.-B.; Medforth, C. J.; Huo, Q.; Pincus, J. L.; Qiu, Y.; Sasaki, D. Y.; Miller, J. E.; Shelnutt, J. A. *Chem. Mater.* **2006**, *18*, 2335−2346.
(14) Wang, H.; Song, Y.; Medforth, C. J.; Shelnutt, J. A. *J. Am. Chem. Soc.* **2006**, *128*, 9284−9285.
(15) Wang, S.; Hori, T. *J. Porphyrins Phthalocyanines* **2003**, *7*, 37−41.

10.1021/ic7016165 CCC: $37.00
Published on Web 11/10/2007

Chart 1

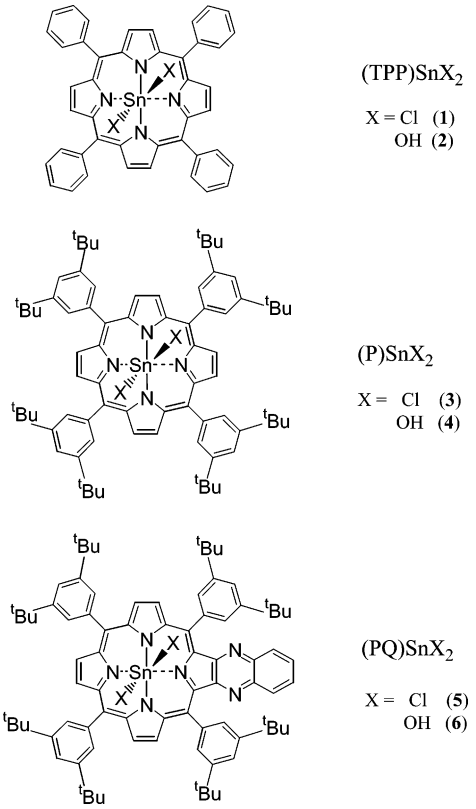

to better understand their function in various applications, and with this in mind, a number of Sn(IV) porphyrins with different macrocycles and coordinated axial ligands have been characterized as to their electrochemistry in nonaqueous media where π-anion radicals and dianions are easily generated.[17−26] The formation of a Sn(IV) π-anion radical occurs at a more positive potential than for all other metalloporphyrins with the same macrocycle,[17,25] with the exact value of $E_{1/2}$ being dependent upon the type of axial ligand and overall basicity of the conjugated macrocycle.[17,18,20−26] The latter can be systematically varied by adding electron-donating or electron-withdrawing substituents to the macrocycle[24,25] or by extension of the π-ring system as in the case of quinoxalinoporphyrins.[30] Although Sn(II) porphyrins are known,[25,31−33] the conversion of Sn(IV) to Sn(II) does not occur under the electrochemical conditions.

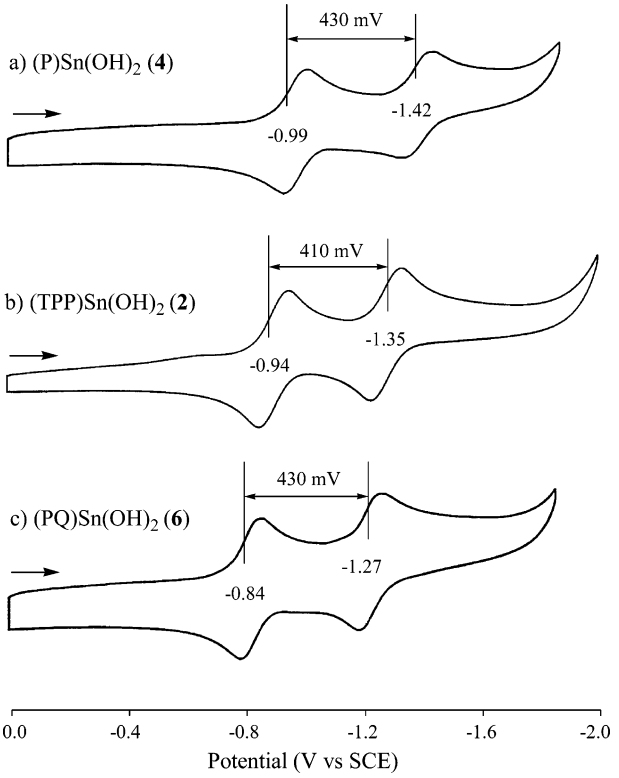

Figure 1. Cyclic voltammograms of (Por)Sn(OH)$_2$ for the reductions in CH_2Cl_2, 0.1 M TBAP.

In the present paper, we have utilized electrochemistry and thin-layer spectroelectrochemistry to elucidate the fate of the electrogenerated products after the electroreduction or electrooxidation of three dichloro- and three dihydroxo-Sn(IV) porphyrins in dichloromethane containing 0.1 or 0.2 M tetra-*n*-butylammonium perchlorate (TBAP) as supporting electrolyte. The examined compounds are shown in Chart 1 and represented as (TPP)SnX$_2$, (P)Sn(X)$_2$, and (PQ)Sn(X)$_2$, where TPP = 5,10,15,20-tetraphenylporphyrin, P = 5,10,15,20-tetrakis(3,5-di-*tert*-butylphenyl)porphyrin, PQ = 5,10,15,-20-tetrakis(3,5-di-*tert*-butylphenyl)quinoxalino[2,3-*b*′]porphyrin, and X = Cl or OH. In some cases, the compounds are represented as (Por)SnX$_2$, where Por is a general porphyrin chelate.

Previous electrochemical and spectroscopic measurements of (TpTP)SnCl$_2$ and (TmTP)SnCl$_2$ in tetrahydrofuran (THF)

(16) Wang, S.; Tabata, I.; Hisada, K.; Hori, T. *J. Porphyrins Phthalocyanines* **2003**, *7*, 199−204.
(17) Fuhrhop, J.-H.; Kadish, K. M.; Davis, D. G. *J. Am. Chem. Soc.* **1973**, *95*, 5140−5147.
(18) Kadish, K. M.; Xu, Q. Y.; Maiya, G. B.; Barbe, J. M.; Guilard, R. *J. Chem. Soc., Dalton Trans.* **1989**, 1531−1536.
(19) Kadish, K. M.; Swistak, C.; Boisselier-Cocolios, B.; Barbe, J. M.; Guilard, R. *Inorg. Chem.* **1986**, *25*, 4336−4343.
(20) Kadish, K. M.; Dubois, D.; Koeller, S.; Barbe, J. M.; Guilard, R. *Inorg. Chem.* **1992**, *32*, 3292−3294.
(21) Felton, R. H.; Linschitz, H. *J. Am. Chem. Soc.* **1966**, *88*, 1113−1116.
(22) Guilard, R.; Barbe, J. M.; Fahim, M.; Atmani, A.; Moninot, G.; Kadish, K. M. *New J. Chem.* **1992**, *16*, 815−820.
(23) Guilard, R.; Ratti, C.; Barbe, J. M.; Dubois, D.; Kadish, K. M. *Inorg. Chem.* **1991**, *30*, 1537−1542.
(24) Reddy, D. R.; Maiya, B. G. *J. Porphyrins Phthalocyanines* **2002**, *6*, 3−11.
(25) (a) Kadish, K. M.; Van Caemelbecke, E.; Royal, G. In *The Porphyrin Handbook*; Kadish, K. M., Smith, K. M., Guilard, R., Eds.; Academic Press: San Diego, CA, 2000; Vol. 8, pp 1−114. (b) Kadish, K. M.; Royal, G.; Van Caemelbecke, E.; Gueletti, L. In *The Porphyrin Handbook*; Kadish, K. M., Smith, K. M., Guilard, R., Eds.; Academic Press: San Diego, CA, 2000; Vol. 9, pp 1−219.
(26) Lemke, F. R.; Lorenz, C. R. *Recent Res. Dev. Electroanal. Chem.* **1999**, *1*, 73−89.
(27) Arnold, D. P. *Polyhedron* **1988**, *7*, 2225−2227.
(28) Hawley, J. C.; Bampos, N. B.; Abraham, R. J.; Sanders, J. K. M. *Chem. Commun.* **1998**, 661−662.
(29) Arnold, D. P.; Blok, J. *Coord. Chem. Rev.* **2004**, *248*, 299−319.
(30) (a) Kadish, K. M.; E, W.; Sintic, P.; Ou, Z.; Shao, J.; Ohkubo, K.; Fukuzumi, S.; Govenlock, L. J.; McDonald, J. A.; Try, A. C.; Cai, Z.; Reimers, J. R.; Crossley, M. J. *J. Phys. Chem. B* **2007**, *111*, 8762−8774. (b) Crossley, M. J.; Sintic, P. J.; Hutchison, J. A.; Ghiggino, K. P. *Org. Biomol. Chem.* **2005**, *3*, 852−865.
(31) Kadish, K. M.; Dubois, D.; Barbe, J. M.; Guilard, R. *Inorg. Chem.* **1991**, *30*, 4498−4501.
(32) Whitten, D. G.; Yau, J. C.; Carroll, F. A. *J. Am. Chem. Soc.* **1971**, *93*, 2291−2296.

Table 1. Half-Wave Potentials (V vs SCE) of (Por)$Sn^{IV}X_2$ Complexes in CH_2Cl_2 Containing 0.1 M TBAP

			oxidation		reduction			
T (°C)	axial ligand (X)	macrocycle (Por)	1st	2nd	1st	2nd	Δred (1st − 2nd)	HOMO−LUMO (eV)
22	OH	TPP		1.46[a]	−0.94	−1.35	0.41	2.43
		P		1.36[b]	−0.99	−1.42	0.43	2.35
		PQ	1.56[c]	1.37[d]	−0.84	−1.27	0.43	2.21
	Cl	TPP		1.44	−0.79	−1.25[c]		2.23
		P		1.36	−0.83	−1.34[c]		2.19
		PQ		1.42	−0.67	−1.15[c,e]		2.09
−75	Cl	TPP	1.88	1.42	−0.73	−1.15	0.42	2.15
		P		1.36	−0.75	−1.21	0.46	2.11
		PQ		1.39	−0.59	−1.03	0.44	1.98

[a] Extra oxidations at values of $E_{pa} = 1.10$ and 1.30 V are also observed. [b] Extra oxidation at $E_{pa} = 1.20$ V is also observed. [c] Peak potential at a scan rate of 0.1 V/s. [d] Extra oxidations at values of $E_{pa} = 1.12$ and 1.29 V are also observed. [e] Two extra reductions at $E_{1/2} = -1.25$ and −1.42 V are also observed (see Figure 3).

where TpTP and TmTP are the dianions of tetra-*p*-tolylporphyrin and tetra-*m*-tolylporphyrin, respectively, have demonstrated that the second electroreductions are followed by dissociation of one axially bound Cl ligand, but this does not occur for the dihydroxo derivatives where the two axial ligands remain coordinated after electron addition on the time scale of the electrochemical experiment.[18] As will be demonstrated in the present paper, the addition of two electrons to (PQ)$SnCl_2$ in CH_2Cl_2 is also followed by a loss of both chloro axial ligands, but the mechanism is more complicated than for the previously studied derivatives in that the initial electrogenerated dianion is converted to (PQ)$Sn(OH)_2$ as well as to a protonated form of the quinoxalinoporphyrin, (PQH)$Sn(OH)_2$, both of which are further electroreduced by two electrons. A protonation of the quinoxaline group on the PQ complexes should be independent of the central metal oxidation state, and this is investigated in the present study for (PQ)Ni^{II} and (PQ)Cu^{II} in benzonitrile with and without protons added to solution in the form of trifluoroacetic acid (TFA).

Experimental Section

Chemicals. Synthesis of the investigated Sn(IV) porphyrins (**1**−**6**) has been reported in the literature.[3] (PQ)Ni and (PQ)Cu were also utilized as reference compounds and were synthesized as earlier described.[34] Absolute dichloromethane (CH_2Cl_2) and TFA were purchased from Aldrich Co. and used as received without further purification. TBAP was purchased from Sigma Chemical or Fluka Chemika Co., recrystallized from ethanol, and dried under vacuum at 40 °C for at least 1 week prior to use.

Instrumentation. Cyclic voltammograms were obtained with an EG&G Princeton Applied Research (PAR) 173 potentiostat/galvanostat. A homemade three-electrode cell was used for these measurements and consisted of a platinum button or glassy-carbon working electrode, a platinum counter electrode, and a homemade saturated calomel reference electrode (SCE). The SCE was separated from the bulk of the solution by a fritted glass bridge of low porosity, which contained the solvent/supporting electrolyte mixture. UV−vis spectroelectrochemical experiments were performed with a home-built thin-layer cell that had a light transparent platinum net working electrode.[35] Potentials were applied and monitored with an EG&G PAR Model 173 potentiostat. Time-resolved UV−vis spectra were recorded with a Hewlett-Packard model 8453 diode array spectrophotometer.

Results and Discusion

Electroreduction of (Por)$Sn(OH)_2$. Figure 1 illustrates cyclic voltammograms for the electroreduction of the three (Por)$Sn(OH)_2$ derivatives in CH_2Cl_2 containing 0.1 M TBAP. The easiest-to-reduce porphyrin is (PQ)$Sn(OH)_2$ (**6**) ($E_{1/2} = -0.84$ and −1.27 V), and the hardest-to-reduce porphyrin is (P)$Sn(OH)_2$ (**4**) ($E_{1/2} = -0.99$ and −1.42 V), with (TPP)-$Sn(OH)_2$ (**2**) ($E_{1/2} = -0.94$ and −1.35 V) in-between in comparison (Table 1), a trend which parallels earlier reported results for divalent metal derivatives of (TPP)M, (PQ)M, and (P)M.[30a,36] Each compound undergoes two reversible one-electron reductions with the absolute potential difference between the processes ranging from 410 to 430 mV as seen in Figure 1. There is no evidence for breaking of the Sn(IV)−OH bonds on the cyclic voltammetry time scale.

Electroreduction of (TPP)$SnCl_2$ and (P)$SnCl_2$. The electrochemistry of (TPP)$SnCl_2$ and (P)$SnCl_2$ differs from that of the three above dihydroxo-tin(IV) porphyrin complexes in CH_2Cl_2 containing 0.1 M TBAP. Although two one-electron reductions can be observed for all of the examined compounds, the second reduction of (TPP)$SnCl_2$ and (P)$SnCl_2$ is reversible only at low temperature, as seen in Figure 2. The absolute potential difference ($\Delta E_{1/2}$) between the first and second electron additions to the two porphyrins at −75 °C is 0.42 V for Por = TPP and 0.46 V for Por = P (Table 1), values similar to those of (Por)$Sn(OH)_2$ (Figure 1) and numerous TPP and TPP-like complexes under similar solution conditions.[25]

The stepwise reductions of (TPP)$SnCl_2$ and (P)$SnCl_2$ in CH_2Cl_2 are both easier than those for reduction of the analogous (TPP)$Sn(OH)_2$ and (P)$Sn(OH)_2$ derivatives by 150−200 mV, and this electrochemical result is consistent

(33) Barbe, J. M.; Ratti, C.; Richard, P.; Lecomte, C.; Gerardin, R.; Guilard, R. *Inorg. Chem.* **1990**, *29*, 4126−4130.
(34) Crossley, M. J.; Sintic, P. J.; Walton, R.; Reimers, J. R. *Org. Biomol. Chem.* **2003**, *1*, 2777−2787.
(35) Lin, X. Q.; Kadish, K. M. *Anal. Chem.* **1985**, *57*, 1498−1501.
(36) Ou, Z.; E, W.; Shao, J.; Burn, P. L.; Sheehan, C. S.; Walton, R.; Kadish, K. M.; Crossley, M. J. *J. Porphyrins Phthalocyanines* **2005**, *9*, 142−151.

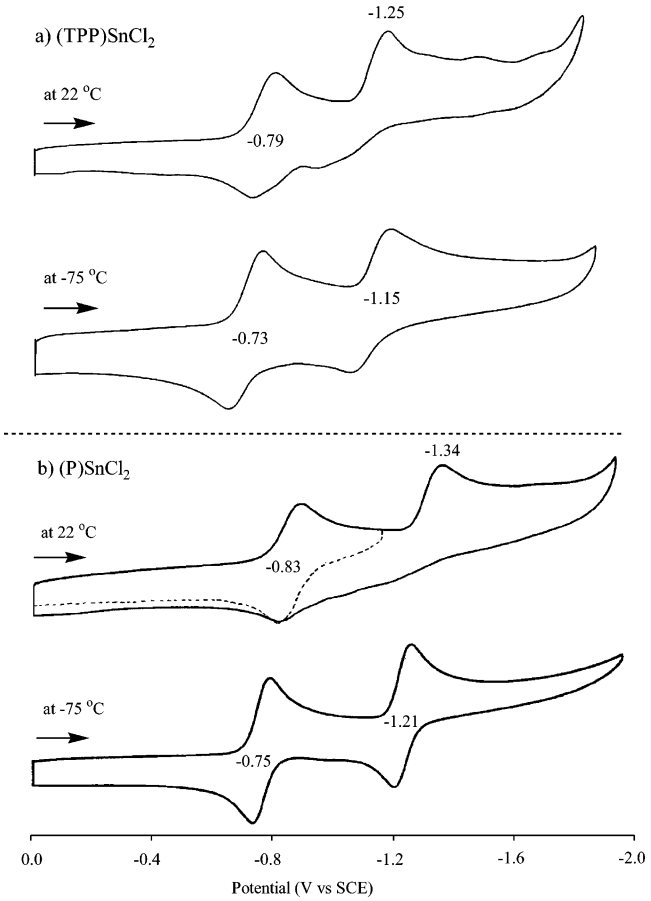

Figure 2. Cyclic voltammograms showing the electroreduction of (a) (TPP)$SnCl_2$ and (b) (P)$SnCl_2$ in CH_2Cl_2, 0.1 M TBAP, at a scan rate of 0.1 V/s.

with a weaker binding of Cl^- to the Sn(IV) center of the neutral and electroreduced porphyrins as compared with that of OH^-. A similar dependence of reduction potentials on the axial ligand was reported earlier for (TpTP)SnX_2 and (TmTP)SnX_2 in THF where X = Cl or OH.[18]

As seen in Figure 2, the second reduction of (TPP)$SnCl_2$ and (P)$SnCl_2$ is irreversible at room temperature and the shape and temperature dependence of the current−voltage curves is indicative of a chemical reaction following electron transfer (an electrochemical EC mechanism). The products of the chemical reaction are electroactive, but none of the redox processes are well-defined in CH_2Cl_2 and they were not investigated in further detail. This differs from what is observed for (PQ)$SnCl_2$ (**5**) where several new and well-defined oxidation and reduction processes can be seen after the formation of a transient Sn(IV) porphyrin dianion as described in the following section.

Electroreduction and Protonation of (PQ)$SnCl_2$. The first one-electron reduction of (PQ)$SnCl_2$ at −75 °C is located at $E_{1/2}$ = −0.59 V (Figure 3a) but is shifted to −0.67 V at room temperature (Figure 3b). Both potentials are 160 mV positive of $E_{1/2}$ values for the reduction of (P)$SnCl_2$ to its π-anion radical at the same temperature (Figure 2b). The separation in half-wave potentials (at −75 °C) between the first and second reversible reductions of (PQ)$SnCl_2$ is 0.44 V (Table 1), which is similar to the $\Delta E_{1/2}$ value for (Por)-$Sn(OH)_2$ (Figure 1) and also consistent with the stepwise

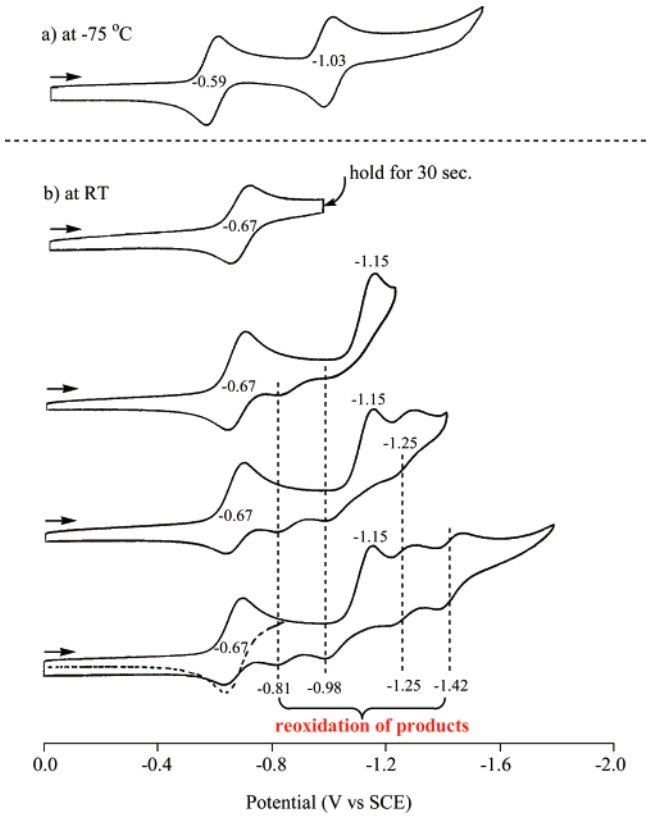

Figure 3. Cyclic voltammograms of (a) (PQ)$SnCl_2$ (**5**) at −75 °C and (b) room temperature (22 °C) in CH_2Cl_2, 0.1 M TBAP.

addition of two electrons to the porphyrin π-ring system. (PQ)$SnCl_2$ is also easier to reduce than (P)$Sn(OH)_2$ by 320 mV in CH_2Cl_2 at room temperature (see Figure 1 and Table 1), thus pointing out the combined influence of the macrocyclic structure (P or PQ) and axial ligand (Cl or OH) in modulating redox potentials for reduction at the conjugated π-ring system of Sn(IV) porphyrins.

Although the formation of π-anion radicals has been observed at reduction potentials in the range of −0.1 to −0.5 V for Sn(IV) porphyrins containing one or two weakly coordinating anions,[18,31] the $E_{1/2}$ value of −0.59 V for the formation of a porphyrin π-anion radical from (PQ)$SnCl_2$ at −75 °C is more positive than the ring-centered reactions of all other metalloporphyrins with PQ, TPP, or P macrocycles and central metal ions in +2, +3, or +4 oxidation states.[25,30a,36]

The first one-electron reduction product of (PQ)$SnCl_2$ is relatively stable at room temperature, as indicated by the fact that this process remains reversible when the scan is held at −0.90 V for 30 s prior to reoxidation (Figure 3b). This contrasts with the second one-electron reduction where the irreversible cathodic peak at E_{pc} = −1.15 V is coupled to two new reoxidation peaks at E_{pa} = −0.81 and −0.98 V and two new reductions at $E_{1/2}$ = −1.25 and −1.42 V for a scan rate of 0.1 V/s. These processes are indicated by dashed lines in Figure 3b, which show the current−voltage curves obtained upon scanning from 0.0 V to progressively more and more negative potentials, thus enabling a monitoring of the products formed in each electron-transfer step.

The voltammetric data in Figure 3 suggests that two distinctly different porphyrin products are formed after the

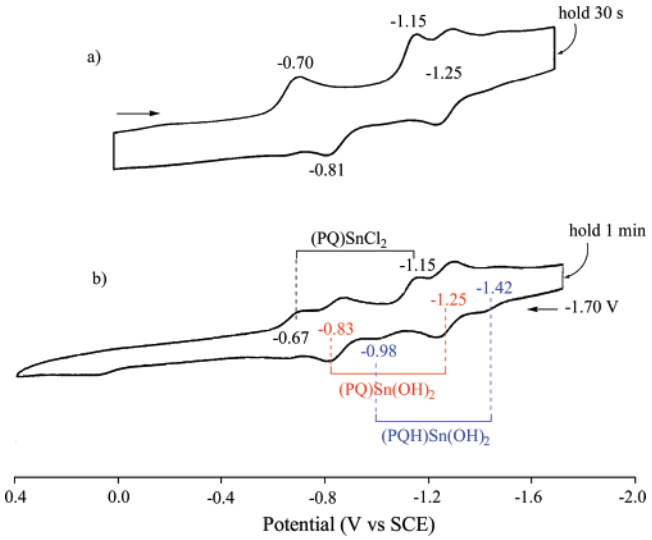

Figure 4. Cyclic voltammograms of $(PQ)SnCl_2$ (**5**) in CH_2Cl_2, 0.1 M TBAP, at a scan rate of 0.1 V/s TBAP with different scan directions.

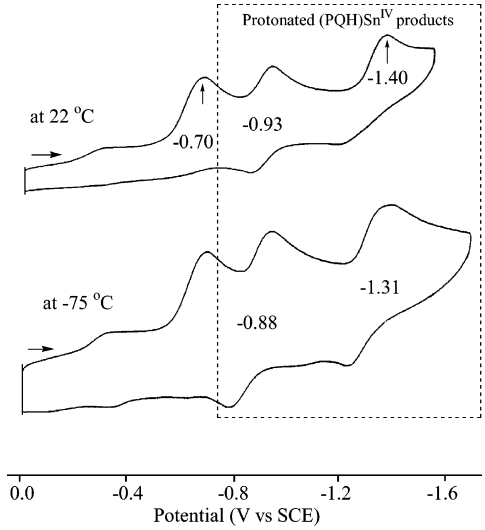

Figure 5. Cyclic voltammograms of $(PQ)SnCl_2$ in CH_2Cl_2 containing 0.1 M TBAP and 5 equiv added TFA.

reduction of $(PQ)SnCl_2$ at −1.15 V, both of which are electroactive and can be further reduced or oxidized in single one-electron-transfer steps. One of the electroreduction products is reduced at $E_{1/2} = -1.25$ V and oxidized at $E_{pa} = -0.81$ V while the other is reduced at $E_{1/2} = -1.42$ V and oxidized at $E_{pa} = -0.98$ V for a scan rate of 0.1 V/s. The potentials for one of the electrogenerated products are virtually identical to the values for the reduction and reoxidation of $[(PQ)Sn(OH)_2]^-$ (see Figure 1c) while the other Sn(IV) porphyrin product has potentials virtually identical to the $E_{1/2}$ values for the reduction and reoxidation of $[(P)Sn(OH)_2]^-$ (Figure 1a). This latter result implies the apparent conversion of $(PQ)SnCl_2$ to $(PQ)Sn(OH)_2$ in the electrochemical cell. This type of reaction is not without precedent in the porphyrin literature[37] and was shown to occur upon the electroreduction of $(OEP)Ge(ClO_4)_2$ or $(TPP)Ge(ClO_4)_2$ where the dihydroxo-Ge(IV)porphyrin was generated at the electrode surface under similar solution conditions. An evaluation of the mechanism involving the exchange of axial ligands showed that a dihydroxo-Ge(IV) porphyrin was formed as a final product after the electroreduction of trace H_2O in the solvent or H_2O axially bound to the porphyrin metal center.[37]

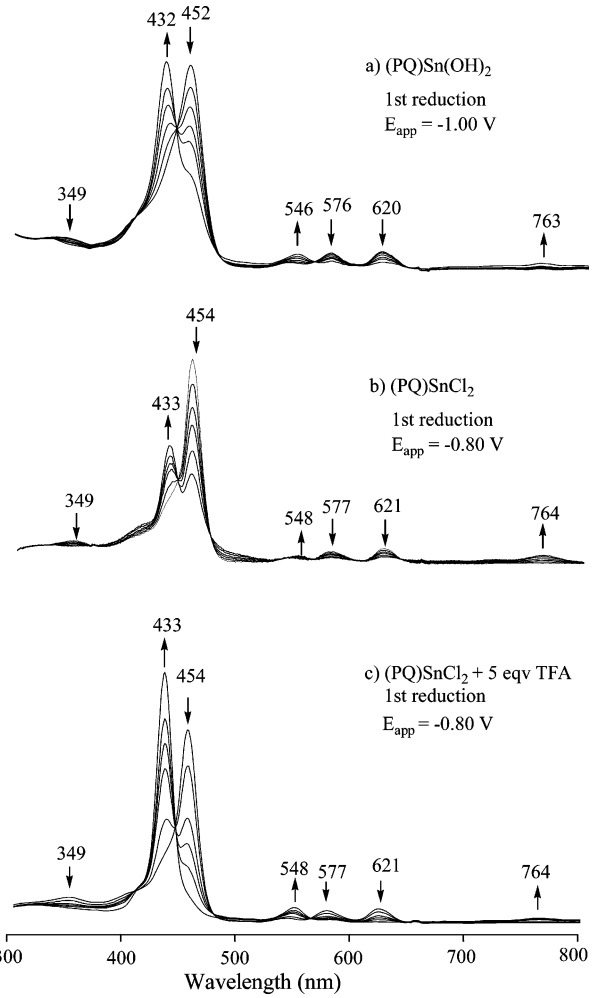

Figure 6. Thin-layer UV−vis spectral changes during the first controlled potential reduction in CH_2Cl_2 containing 0.2 M TBAP for (a) $(PQ)Sn(OH)_2$, (b) $(PQ)SnCl_2$, and (c) $(PQ)SnCl_2$ containing 5 equiv added TFA.

The similarity between potentials for the reduction and reoxidation of genuine $[(P)Sn(OH)_2]^-$ ($E_{1/2} = -1.42$ and −0.99 V) and the products of the $(PQ)SnCl_2$ second reduction ($E_{1/2} = -1.42$ and −0.98 V) can also be easily explained by considering that a liberated proton produced during the formation of the dihydroxo-tin(IV) complex is added to the quinoxaline group (Q), thus leading to $(PQH)Sn(OH)_2$ at the electrode surface. A protonation of the Q group evidently interferes with the conjugation between the fused quinoxaline unit and the porphyrin macrocycle, thus effectively giving a compound whose reduction properties resemble that of the metalloporphyrin in the absence of the fused ring. Under these conditions, both $(PQ)Sn(OH)_2]^-$ and $(PQH)Sn(OH)_2$ would be generated in solution after the reduction of $(PQ)SnCl_2$ at −1.15 V. To further investigate this possibility, cyclic voltammograms were obtained under experimental conditions where the dihydroxo products were generated at a controlled negative potential and the products then oxidized

(37) Kadish, K. M.; Xu, Q. Y.; Barbe, J. M.; Anderson, J. E.; Wang, E.; Guilard, R. *Inorg. Chem.* **1988**, *27*, 691−696.

Scheme 1. Proposed Electroreduction Mechanism and Protonation of $(PQ)SnCl_2$ in CH_2Cl_2, 0.1 M TBAP, on the Cyclic Voltammetry Time Scale

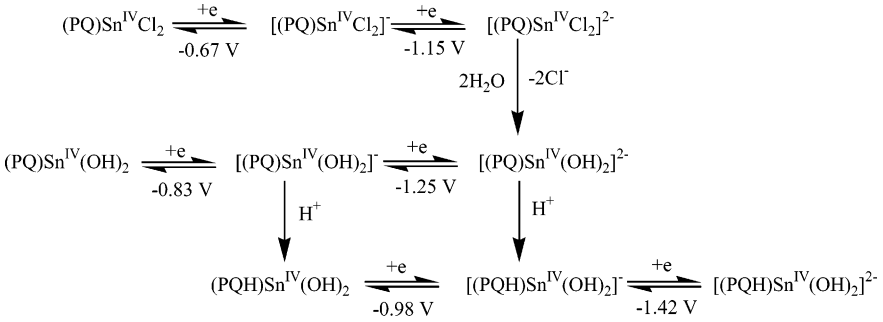

by scanning in a positive direction. In one experiment, the potential was scanned from 0.0 to −1.60 V and then held for 30 s at −1.60 V prior to changing the scan direction and reoxidizing the products of the electroreduction and/or coupled chemical reaction (Figure 4a). Under these experimental conditions, the new redox processes at $E_{1/2} = -1.25$ V and $E_{pa} = -0.81$ V are both well-defined and have about equal peak currents for electrooxidation. The currents for the new reduction process at $E_{1/2} = -1.42$ V and the new reoxidation peak at −0.98 V are also about equal to each other, but both are much decreased in magnitude compared with what is observed in Figure 3 where the final product of $(PQ)SnCl_2$ electroreduction can be formulated as almost exclusively $[(PQ)Sn(OH)_2]^{2-}$ based on the $E_{1/2}$ values of −1.25 and −0.84 V.

The same chemical products are produced when the negative potential scan is initiated at −1.70 V after holding the potential at this value for 1 min prior to making the electrochemical measurement. A cyclic voltammogram obtained under these experimental conditions is illustrated in Figure 4b where the reoxidations attributed to $(PQ)Sn(OH)_2$, $(PQH)Sn(OH)_2$, and $(PQ)SnCl)_2$ are indicated by dashed lines highlighting the two redox processes of each species.

The assignments of each redox process in Figures 3 and 4 to a specific compound are self-consistent, and a proposed mechanism for the conversion of $(PQ)SnCl_2$ to both $(PQ)Sn(OH)_2$ and $(PQH)Sn(OH)_2$ is given in Scheme 1, which includes the reversible $E_{1/2}$ values for each electron-transfer process. At −75 °C, only $[(PQ)SnCl_2]^-$ and $[(PQ)SnCl_2]^{2-}$ are generated in solution, but at room temperature, there is a rapid formation of $[(PQ)Sn(OH)_2]^-$, which can be oxidized by one electron to give neutral $(PQ)Sn(OH)_2$, reduced by one electron to give the porphyrin dianion $[(PQ)Sn(OH)_2]^{2-}$, or protonated to give $(PQH)Sn(OH)_2$. The protonated porphyrin is electroactive and undergoes stepwise one-electron reductions at $E_{1/2} = -0.98$ and −1.42 V vs SCE, potentials virtually identical to those for reduction of the "simple" dihydroxo-tin(IV) porphyrin in the absence of a fused quinoxaline group, i.e., $(P)Sn(OH)_2$, where $E_{1/2} = -0.99$ and −1.42 V (Figure 1a).

It is important to point out that a protonation of the quinoxaline group in neutral $(PQ)SnCl_2$ does not occur in CH_2Cl_2, 0.1 M TBAP, nor does it occur upon formation of the anion radical in this solvent on the cyclic voltammetry time scale. As seen by cyclic voltammetry, the protonation only occurs upon the formation of doubly reduced $(PQ)SnCl_2$ and is facilitated by a reaction of the electrogenerated dianion with trace H_2O in solution, leading to the formation of OH^-, which coordinates to the metal center, and H^+, which adds to the quinoxaline group as indicated in
Scheme 1.

As described above, the electrogenerated $[(PQ)SnCl_2]^-$ is stable in CH_2Cl_2 containing 0.1 M TBAP on the cyclic voltammetric time scale. However, the monoanion rapidly protonates after acid is added to solution in the form of TFA, and this results in an irreversible reduction at $E_{pc} = -0.70$ V followed by two one-electron-transfer steps at $E_{1/2} = -0.93$ V and $E_{pc} = -1.40$ V for a scan rate of 0.1 V/s (Figure 5). The latter process becomes reversible at lower temperatures, and at −75 °C the two reductions are located at $E_{1/2} = -0.88$ and −1.31 V (Figure 5) as compared with $E_{1/2} = -0.59$ and −1.03 V for reduction of the original $(PQ)SnCl_2$ at −75 °C in the absence of added acid (Figure 3a).

The two reductions of the protonated product, assigned as $(PQH)SnX_2$, are separated by 430 mV, as all of the other investigated porphyrins in CH_2Cl_2 (Table 1), but the exact nature of the axial ligands (X) cannot be definitively assigned on the basis of the measured redox potentials. The reversible room-temperature reduction of $(PQH)SnX_2$ ($E_{1/2} = -0.93$ V) is 50 mV lower than the $E_{1/2}$ value for the room-temperature reduction of $(PQH)Sn(OH)_2$ (−0.98 V), but is more negative than the $E_{1/2}$ value for the reduction of $(P)SnCl_2$ in CH_2Cl_2 (−0.83 V, Figure 2b), thus suggesting a mixture of two different axial ligands on $(PQH)SnX_2$, Cl, and OH, for example. Such chloro-hydroxo-tin(IV) porphyrins can be isolated during the chemical conversion of dichloro-tin(IV) porphyrins to their corresponding dihydroxo-derivatives.[3] Other possible axial ligands are ClO_4^- from the TBAP supporting electrolyte and CF_3COO^-, which would come from the added TFA.

Spectroelectrochemistry of $(Por)SnX_2$. In order to confirm the protonation of the electrogenerated Sn(IV) quinoxalinoporphyrins, UV−vis spectra were measured in a thin-layer cell during the controlled potential reduction of $(PQ)SnX_2$ and $(P)SnX_2$, where X = Cl or OH. The resulting spectral changes are shown in Figure 6 for $(PQ)Sn(OH)_2$ and $(PQ)SnCl_2$ and in Figure S1 (Supporting Information) for $(P)Sn(OH)_2$ and $(P)SnCl_2$. The UV−visible spectra obtained after the first reduction of $(P)SnX_2$, X = OH or Cl (Figure S1), have decreased intensity Soret and Q bands as expected for the formation of a porphyrin π-anion radical. There is a

broad band in the near-IR region of the spectrum, which is located at 747 nm (X = OH) or 739 nm (X = Cl), also indicating the formation of Sn(IV) π-anion radicals. These spectral changes upon the reduction of (P)Sn(OH)$_2$ and (P)SnCl$_2$ are consistent with the electrochemical data described earlier but contrast, in part, with the spectral changes obtained after the first reduction of (PQ)Sn(OH)$_2$ and (PQ)SnCl$_2$ under the same solution conditions (parts a and b of Figures 6). The two reduced PQ derivatives both exhibit a broad 763−764 nm band in the near-IR region of the spectrum, suggesting a π-anion radical formation. Both electroreduced compounds also have decreased intensity Q bands, further indicating a porphyrin π-anion radical. However, unlike reduced (P)SnX$_2$ (Figure S1, Supporting Information), the reduced (PQ)SnX$_2$ derivatives have a well-defined Soret band at 432−433 nm, which is almost exactly the same wavelength as that for the Soret band of (P)SnX$_2$, where λ_{max} = 430 nm (X = OH) or 432 nm (X = Cl) under the same solution conditions. The final spectrum after the reduction of (PQ)Sn(OH)$_2$ has bands at 432, 546, and 763 nm (Figure 6a) and is assigned to the protonated porphyrin (PQH)Sn(OH)$_2$ which is generated as shown in eq 1.

$$(PQ)Sn(OH)_2 \overset{+e}{\rightleftharpoons} [(PQ)Sn(OH)_2]^- \xrightarrow{+H^+} (PQH)Sn(OH)_2 \qquad (1)$$

It should be pointed out that the proposed (PQH)Sn(OH)$_2$ species not only has the same Soret band as (P)Sn(OH)$_2$ but it also has the same half-wave potentials as those for reduction of this "simple" porphyrin without a fused quinoxaline ring, as discussed in earlier sections of this manuscript.

Similar spectral changes are observed upon the controlled potential reduction of (PQ)SnCl$_2$ in CH$_2$Cl$_2$, 0.2 M TBAP, and the first electrogenerated species has bands at 433, 548, and 764 nm (Figure 6b). The initial electroreduction product in this case is assigned as (PQH)SnX$_2$, where X is most likely Cl, OH, or a mixture of the two ligands as concluded on the basis of the redox potentials and discussed above.

The spectroelectrochemical results in parts a and b of Figures 6 for (PQ)Sn(OH)$_2$ and (PQ)SnCl$_2$ are self-consistent, indicating the formation of a protonated porphyrin from the monoanion, and this differs from what is observed by regular cyclic voltammetry where the measurements are made at scan rate of 0.1 V/s, much faster than the time scale of the spectroelectrochemistry measurement (200s). Thus, the monoanions of (PQ)SnCl$_2$ and (PQ)Sn(OH)$_2$ are both stable on the cyclic voltammetry time scale but react on the slower time scale of thin-layer spectroelectrochemistry.

Finally, the spectroelectrochemistry of (PQ)SnCl$_2$ was also carried out in CH$_2$Cl$_2$ solutions with added TFA to spectrally characterize the product of the irreversible first reduction in Figure 5. The resulting spectral changes under these solution conditions are illustrated in Figure 6c. As seen in this figure, upon the application of an applied potential of −0.80 V, the initial UV−vis spectrum of (PQ)SnCl$_2$ (λ_{max} = 454, 577, and 621 nm) is converted to a spectrum with an intense Soret band at 433 nm, a Q-band at 548 nm, and a weak absorption at 764 nm. Again, the Soret band of the (PQH)SnX$_2$ reduction product in Figure 6c is virtually identical to the Soret band position of (P)SnX$_2$, where X = Cl or OH, both of which are located at 432 nm. The electrochemical and spectroelectrochemical results in acidic media are therefore self-consistent and indicate the rapid conversion of (PQ)SnCl$_2$ to a protonated (PQH)SnX$_2$ form of the porphyrin in CH$_2$Cl$_2$.

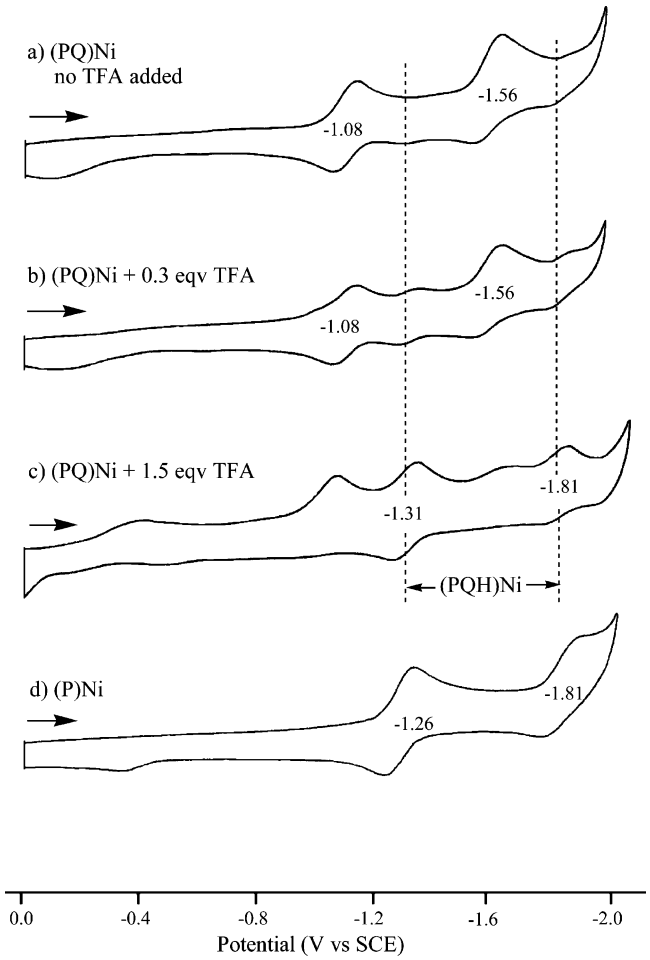

Figure 7. Cyclic voltammograms of (a) (PQ)Ni, (b) (PQ)Ni with 0.3 equiv TFA, (c) (PQ)Ni with 1.5 equiv TFA, and (d) (P)Ni in PhCN containing 0.1 M TBAP.

Electrochemistry of (PQ)Ni and (PQ)Cu with Added TFA. A facile protonation of the fused quinoxaline ring should also occur for reduced quinoxalinoporphyrins with central metal ions in oxidation states other than 2+ and this was demonstrated in the present study by examining the protonation in benzonitrile for two previously investigated quinoxalinoporphyrins, which have been well-characterized in the literature,[30a,36] (PQ)Cu^{II} and (PQ)Ni^{II}. It was expected that the electrogenerated dianion, [(PQ)M]$^{2-}$, would be converted to [(PQH)M]$^-$, as observed for doubly reduced (PQ)SnCl$_2$, and it was also expected that (PQH)M^{II} could be generated from [(PQ)M^{II}]$^-$ by adding protons to solution in the form of TFA.

This is exactly what is seen as illustrated by the cyclic voltammograms in Figures 7 and 8. (PQ)Ni is reduced at $E_{1/2}$ = −1.08 and −1.56 V in freshly distilled PhCN while the protonated form of the compound is generated in solutions containing 0.3−1.5 equiv TFA and is reduced at

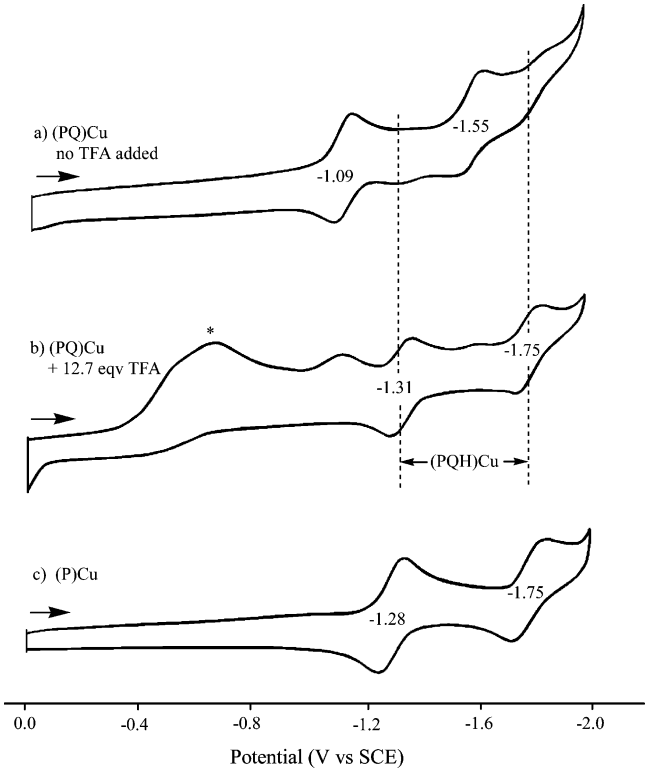

Figure 8. Cyclic voltammograms of (a) (PQ)Cu, (b) (PQ)Cu with 12.7 equiv TFA, and (c) (P)Cu in PhCN containing 0.1 M TBAP. Peaks marked by an asterisk are due to a reduction of excess acid in solution.

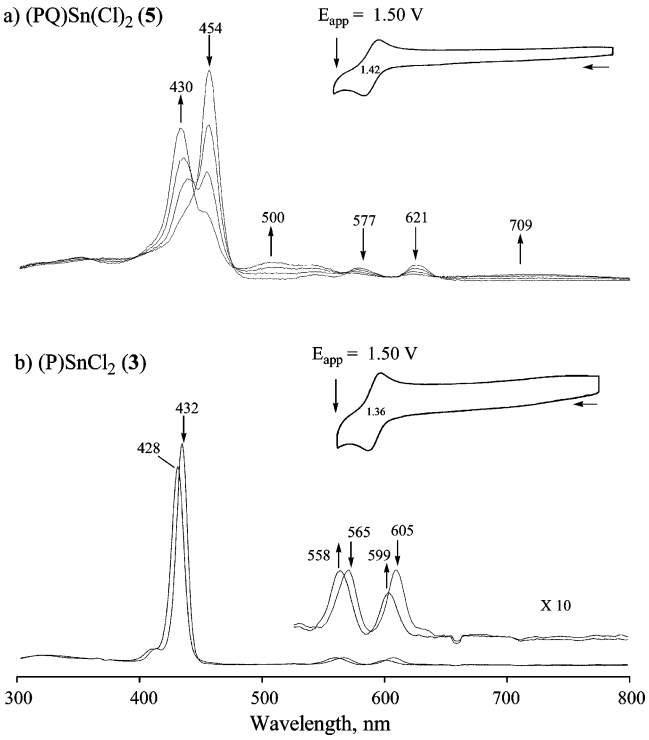

Figure 9. Thin-layer UV−vis spectral changes of (PQ)$SnCl_2$ and (P)-$SnCl_2$ obtained during the controlled potential oxidation in CH_2Cl_2 containing 0.2 M TBAP. Inset shows cyclic voltammograms for oxidation at a scan of 0.1 V/s.

$E_{1/2} = -1.31$ and -1.81 V (Figure 7), values quite close to those for the reduction of (P)Ni in PhCN containing only the supporting electrolyte, 0.1 M TBAP ($E_{1/2} = -1.26$ and -1.81 V). In a similar manner, (PQ)Cu is reduced at $E_{1/2} =$

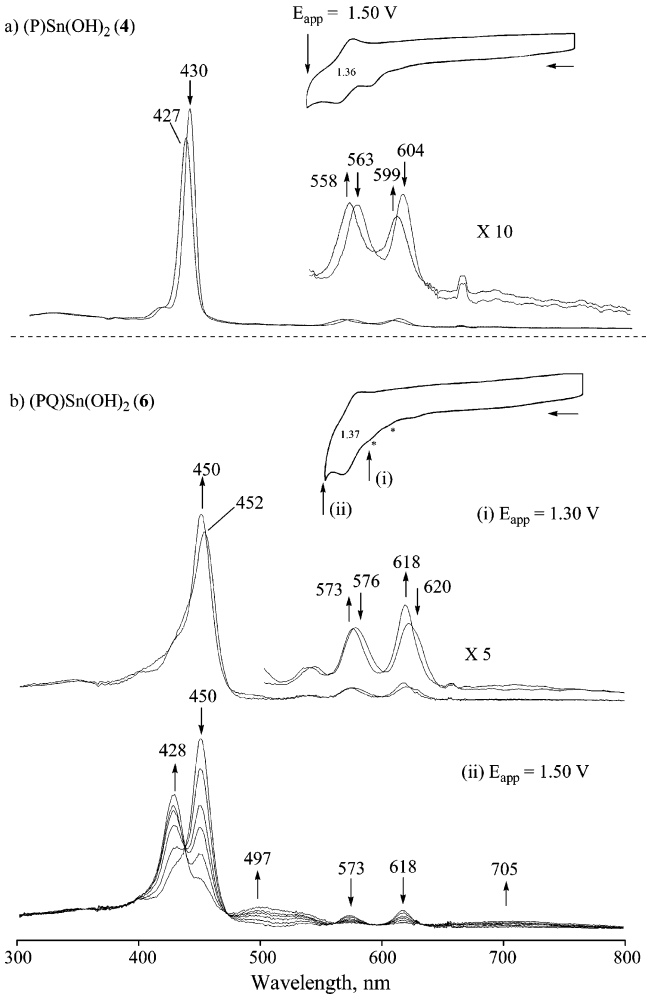

Figure 10. Thin-layer UV−vis spectral changes of (a) (P)$Sn(OH)_2$ and (b) (PQ)$Sn(OH)_2$ obtained during the controlled potential oxidation in CH_2Cl_2 containing 0.2 M TBAP. Insets show cyclic voltammograms for oxidation at a scan of 0.1 V/s.

-1.09 and -1.55 V in freshly distilled PhCN while the protonated form of the compound in PhCN containing TFA is reversibly reduced at $E_{1/2} = -1.31$ and -1.75 V, again, values quite close to the reversible reduction potentials for the reduction of (P)Cu in PhCN not containing any added acid (Figure 8c). Thus, the overall reduction and protonation of $(PQ)M^{II}$ is proposed to occur as shown by the series of reactions given in Scheme 2. The addition of TFA results in a facile protonation of the electrogenerated quinoxalinoporphyrin monoanion while the protonation of the Q group from trace H_2O in freshly distilled PhCN only occurs upon the formation of the more reactive doubly reduced porphyrin.

Electrooxidation of (P)SnX_2 and (PQ)SnX_2. Numerous papers have been published on the reduction of tin(IV) porphyrins,[17−26] but there is very little information in the literature on the electrooxidation of these types of compounds. In fact, to our knowledge, the present study provides the first reported data for the oxidation of Sn(IV) porphyrins having TPP or TPP-like structures with Cl or OH axial ligands.

As seen in Table 1, the room-temperature oxidation of (P)$SnCl_2$ is located at $E_{1/2} = 1.36$ V while (PQ)$SnCl_2$ is oxidized at $E_{1/2} = 1.42$ V as compared to $E_{1/2} = 1.36$ and

Scheme 2. Proposed Electroreduction Mechanism and Protonation of (PQ)Ni and (PQ)Cu on the Cyclic Voltammetry Time Scale in PhCN with and without Added TFA

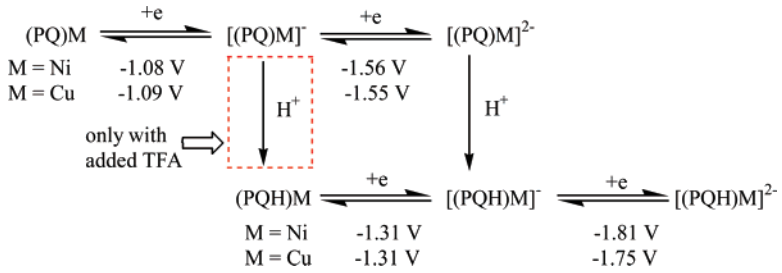

1.37 V for the oxidation of (P)Sn(OH)$_2$ and (PQ)Sn(OH)$_2$ under the same solution conditions. There are also additional irreversible oxidation peaks for the three dihydroxo-tin(IV) porphyrins located at potentials negative to those of the reversible processes, and these can be assigned as a reversible oxidation of free or coordinated hydroxide anion in solution, as verified by independent measurements of TBAOH under the same experimental conditions, where E_p ranges from 1.2 to 1.4 V depending upon the concentration of OH^- (see example of cyclic voltammetry in Figure S2, Supporting Information).

Previous electrochemical studies of (PQ)M, where M = Zn^{II}, Cu^{II}, Ni^{II}, or Pd^{II}, have shown that the fused quinoxaline ring has little or no effect on the oxidation potentials as compared with the $E_{1/2}$ values for the oxidation of (P)M^{II} derivatives having the same central metal ion.[30a,36] This leads to a smaller HOMO−LUMO gap for compounds in the PQ series, which are easier to reduce than the (P)M^{II} derivatives with the same central metal ion. This is also the case for the Sn(IV) porphyrins investigated in the present study where the HOMO−LUMO gap depends on the macrocycle and decreases in the following order: (TPP)SnX_2 > (P)SnX_2 > (PQ)SnX_2. The measured HOMO−LUMO gap also varies as a function of the axial ligands, and for the three series of macrocycles the order is (Por)Sn(OH)$_2$ > (Por)$SnCl_2$. The smallest measured gap is 1.98 V for (PQ)$SnCl_2$ at −75 °C, and the largest is 2.43 V for (TPP)Sn(OH)$_2$ at room temperature (see Table 1).

The first one-electron oxidations of (P)$SnCl_2$ and (PQ)$SnCl_2$ are both reversible and well-defined on the cyclic voltammetry time scale (see inset of Figure 9), and they also have similar $E_{1/2}$ values. Thus, one might reasonably expect both porphyrins to undergo similar mechanisms to give, in each case, a Sn(IV) porphyrin π-cation radical as the product of the first oxidation. Surprisingly, this is not the case for both compounds, as shown by a monitoring of the UV−vis spectra during oxidation at a controlled positive potential in a thin-layer cell.

The UV−vis spectrum obtained after the oxidation of (PQ)$SnCl_2$ at an applied potential of 1.50 V in CH_2Cl_2 (Figure 9a) is consistent with expectation and can be assigned as a porphyrin π-cation radical on the basis of the decreased intensity Soret and Q bands and the appearance of a broad "radical marker band" between 650 and 800 nm in the spectrum (centered in this case at ∼709 nm). In contrast, a radical-like spectrum is not observed upon the oxidation of (P)$SnCl_2$ at the same potential (Figure 9b). In this case, the initial (P)$SnCl_2$ has a Soret band at 432 nm, and two Q bands at 565 and 605 nm while the product of the electrooxidation has almost exactly the same spectral shape and absorption intensity but with all bands blue-shifted by 4−7 nm, giving a species with maximum absorptions at 428, 558, and 599 nm. A comparison of the two spectra in Figure 9b indicates a loss of chloride upon oxidation giving (P)Sn(ClO_4)$_2$, where ClO_4^- comes from the supporting electrolyte. Chloride anion in CH_2Cl_2 is oxidized at potentials between 1.0 and 1.3 V vs SCE (see Figure S2, Supporting Information), and this would be a driving force for the conversion of (P)$SnCl_2$ to $[(P)Sn]^{2+}$ and then (P)Sn(ClO_4)$_2$ as Cl^- is oxidized and ClO_4^- from the supporting electrolyte axially binds to the central metal to neutralize the positive charge of the porphyrin.

Evidence for the formation of a (P)Sn(ClO_4)$_2$ oxidation product from (P)$SnCl_2$ is also based on published UV−vis spectra for related Sn(IV) porphyrins with different anions,[18] where absorption bands of the (P)Sn(ClO_4)$_2$ derivatives are all blue-shifted by 3−9 nm from the same bands of the (P)Sn(Cl)$_2$ species, exactly what is observed in Figure 9b upon electrooxidation at 1.50 V.

An oxidation of the axial ligand also seems to occur for (P)Sn(OH)$_2$, as seen in Figure 10a. Here, the neutral porphyrin is characterized by a Soret band at 430 nm and two Q bands at 563 and 604 nm while the final oxidation product has a Soret band at 427 nm and two Q bands at 558 and 599 nm. The latter spectrum is virtually the same as that obtained after the oxidation of (P)$SnCl_2$, and this suggests the same (P)Sn(ClO_4)$_2$ porphyrin oxidation product in each case.

In a similar manner, the irreversible oxidation of (PQ)Sn(OH)$_2$ at an applied potential of 1.30 V (Figure 10b) seems to only involve the hydroxo ligand (see Figure S2, Supporting Information), giving (PQ)Sn(ClO_4)$_2$, and this reaction is followed by the generation of the expected π-cation radical $[(PQ)Sn(ClO_4)_2]^{\bullet+}$ at a more positive applied potential of 1.50 V. The final UV−vis spectrum after the oxidation of (PQ)Sn(OH)$_2$ at 1.50 V (Figure 10b) is almost the same as that for electrooxidized (PQ)$SnCl_2$ at the same potential (Figure 9a), and this suggests the same form of the porphyrin in solution, namely, a Sn(IV) porphyrin π-cation radical.

It is known that metalloporphyrins with perchlorate ligands are often harder to oxidize than the related chloro or hydroxo forms of the molecules,[25] and the formation of a Sn(IV) porphyrin π-cation radical upon the oxidation of (P)Sn(ClO_4)$_2$ is therefore expected to occur at a more positive

potential than that for the oxidation of the neutral $(P)Sn(OH)_2$ or $(P)SnCl_2$. The electrogenerated $(P)Sn(ClO_4)_2$ is not further oxidized in CH_2Cl_2 at an applied potential of 1.50 V, thus suggesting a much more positive $E_{1/2}$ value for $(P)Sn(ClO_4)_2$ oxidation as compared with that of $(PQ)Sn(ClO_4)_2$, which can be converted to its π-cation radical form within the positive potential limit of the solvent.

In summary, the electrochemistry of the six investigated Sn(IV) porphyrins demonstrates how changes in oxidation/reduction mechanisms and the site of electron transfer can vary significantly with changes in both the axial ligands and the macrocycle. The three dihydroxo-tin(IV) porphyrins are all reduced at the conjugated π-ring system to give stable π-anion radical and dianions. However, this is not the case for the three dichloro-tin(IV) porphyrins where the chloro ligands are labile in the electrogenerated dianions, and these species are highly reactive, leading to several reaction products which were characterized as $(PQ)Sn(OH)_2$ and $(PQH)Sn(OH)_2$ in the case of the quinoxalinoporphyrins. Several reaction products are also observed upon electrooxidation, with the spectroelectrochemistry indicating a conversion of the bis-OH or bis-Cl derivatives to their perchlorate forms prior to the formation of Sn(IV) π-cation radicals. This has not previously been reported in the literature and is not evident from analysis of the reversible cyclic voltammograms alone.

Acknowledgment. The support of the Robert A. Welch Foundation (K.M.K, Grant E-680) and the Jiangsu University Foundation (05JD6051) are gratefully acknowledged. This work was also partially supported by a Discovery Research Grant (DP0208776) from the Australian Research Council. Dr. Jianguo Shao is acknowledged for his help in early electrochemical measurements.

Supporting Information Available: Figures S1 (thin-layer spectral changes) and S2 (cyclic voltammograms) in PDF format. This material is available free of charge via the Internet at http://pubs.acs.org.

IC7016165